Weak forces at work in dye-loaded zeolite materials: spectroscopic investigation on cation–sulfur interactions†

Giorgio Macchi,*[a] Chiara Botta,[b] Gion Calzaferri,[c] Michele Catti,[a] Jérôme Cornil,[d] Johannes Gierschner,[e] Francesco Meinardi[a] and Riccardo Tubino[a]

The interaction between sulfur-containing chromophores and cationic species (K^+) has been investigated in dye-loaded zeolite materials by means of photoluminescence spectroscopy. A red-shift in the emission spectra of the host–guest compounds (HGCs) has been detected and unambiguously connected to the close proximity between a conjugated moiety and nearby free charges, suggesting a specific role played by sulfur lone pair electrons. Quantum-chemical calculations on model compounds have been performed to support this hypothesis.

Introduction

Weak interactions play a fundamental role in many scientific areas, spanning from chemistry and biology to physics and materials science, as well as in technological fields like molecular electronics and nanotechnology. Non-bonding forces (*e.g.* hydrogen bonds, van der Waals interactions, *etc.*) determine the captivating supramolecular architectures of nature's functional structures in living cells, providing us a challenging paradigm for the design of new devices.

The interaction between alkali metal cations and π-conjugated moieties has been recognized as one of the weak forces defining the supramolecular architecture of biological systems.[1–4] Experimental studies on small molecules in the gas phase revealed this effect, but only recent observations in condensed phases have led to a more detailed investigation of all its manifestations, from small molecular complexes to large, multi-subunit protein systems. As an instrument of molecular recognition, cation–π interactions have been detected in many biological systems, such as amino–aromatic interactions in proteins, the binding of acetylcholine and related ligands, catalysis-assisted dealkylation of sulfonium ions and of cyclase reactions in steroid biosynthesis, selectivity of K^+ channels and ligand binding in proteins.[1] Cation–π interactions between counterions in zeolites and arenes (*e.g.* benzene, toluene) were identified by means of infrared spectroscopy,[3] suggesting a charge density correlation for the interaction.[5] Both experimental and theoretical approaches on the subject are focused on the stability of ion–molecule complexes or on the calculation of binding energies, providing relative trends with respect to the cation and to the aromatic or conjugated moiety. A small number of papers dealing with the effect of such an interaction on the photophysical properties of organic chromophores are present in the literature: interaction between metal oxide surfaces,[6–8] as well as oxide porous hosts with functional groups or atoms of dye molecule has been reported to influence the electronic spectra of chromophores,[9] whereas Hashimoto *et al.* reported that the optical properties of oligoacenes are basically unaffected by the close proximity of charged ions.[2,10] The influence of the proton activity inside the channels of zeolite L has been discussed recently.[11,12] The influence of the co-cations is especially important in absence of any solvent inside of the channels, *e.g.* a very high phosphorescence yield due to the pronounced heavy atom effect.[13,14] Though a quite large number of chromophores have been loaded into zeolites by Calzaferri *et al.*,[15] to the best of our knowledge, the specific interaction between cations and sulfur-rich dyes such as oligothiophenes (OTs) has not been thoroughly investigated.

Within this line of thought, channel-forming materials with small channel diameter are attractive to investigate molecular interactions at work, due to both defined geometrical parameters and chemical environment inside the channels that allow for a detailed study of the properties of isolated or weakly interacting molecules.[15–18] Different to all-organic host–guest compounds (HGCs) which typically use unspecific host materials, *i.e.* saturated hydrocarbons,[19] microporous materials such as zeolite L or AlPO-5 allow for the investigation of specific interactions with neighbouring species of the surrounding host framework.[20,21]

The aim of this work is to study the photoluminescence (PL) properties of zeolite-based HGCs loaded with small conjugated molecules, in order to elucidate the role of cation–chromophore interactions on the emissive behaviour of the material. In particular, we focus our attention on sulfur-containing π-conjugated molecules (such as OTs) in which the larger polarizability of S atoms is expected to play a prominent role for chromophore–cation interactions. We demonstrate how

[a] *Università degli Studi di Milano Bicocca and INFM, Dipartimento di Scienza dei Materiali, via R.Cozzi 53, I-20125 Milano, Italy. E-mail: giorgio.macchi@mater.unimib.it*
[b] *Istituto per lo Studio delle Macromolecole, CNR, via Bassini 15, I-20133 Milano, Italy*
[c] *Department of Chemistry and Biochemistry, Universität Bern, Freiestrasse 3, 3012 Bern, Switzerland*
[d] *Laboratory for Chemistry of Novel Materials, University of Mons, Place du Parc 20, B-7000 Mons, Belgium*
[e] *Madrid Institute for Advanced Studies IMDEA Nanoscience, Modulo C-IX, Av. Tomás y Valiente 7, Campus de Cantoblanco, 28049 Madrid, Spain*
† Electronic supplementary information (ESI) available: Experimental, results, discussion and Figures. See DOI: 10.1039/b919880f

charge–molecule interaction affects the photophysics of the prepared hybrid materials, by tuning its PL with a large red shift of the emission spectrum.

Experimental

We have prepared HGCs with various host matrices as well as different organic chromophores (see Scheme 1) in order to connect the occurrence of peculiar optical behavior in the HGC compared with the isolated molecule and to the solid state.
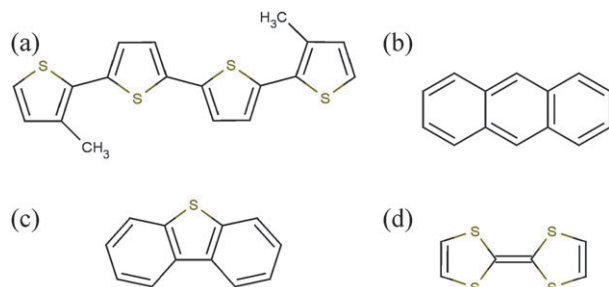
Materials

3,3‴-Dimethylquaterthiophene (DM4T) has been synthesized in accordance with literature.[22] Anthracene (ANT, puriss., $\geq$ 99.0%) and dibenzothiophene (DBT, 99.4%) were purchased at Sigma-Aldrich and used as received (see Scheme 1 for structural formulae).

Zeolite L (LTL) with the stoichiometry $K_9(AlO_2)_9(SiO_2)_{27} \times$ 21 H_2O (molar mass of a unit cell = 2883 g mol^{-1}, 2505 g mol^{-1} dehydrated, cylindrical crystals with a diameter of 0.6 μm and a height of 0.6 μm), microporous titanosilicate ETS-10 polymorph A (ETS, stoichiometry $(Na_{12}K_4)Si_{40}Ti_8O_{104}$) and aluminophosphate AlPO-5 (AlPO-5, cylindrical crystals with a diameter of 1.0 μm and 2.0 μm height) were synthesized according to the recipes detailed in the literature.[23–25]

From here on, HGCs will be referred using acronyms derived as follows: the name of the guest-name of the host-preparation details (*e.g.* DM4T-LTL-L means LTL loaded with DM4T at low concentration).

HGC preparation

Dye-loaded porous materials have been prepared following the double ampoule method described in the literature.[26] In a typical synthesis, 200 mg of the host were dehydrated in mild vacuum (0.03 Torr) for 6 h at 673 K. The guest was degassed at room temperature in mild vacuum (0.03 Torr) for 1 h. Inclusion of the guest species took place in a standard tubular furnace where the gradient in the oven helps to direct the sublimation of the dye in the host-containing chamber. Periodic rotation of the ampoule secured a homogenization of the sample. The relative amount of chromophore in the guest-containing chamber determines the *nominal* number of sites occupied by the guest within the host channels. Except for one case (see below), the glass ampoule was broken and the

Scheme 1 Structural formulae of (a) 3,3‴-dimethyl-quaterthiophene (DM4T), (b) anthracene (ANT), (c) dibenzo-thiophene (DBT) and (d) tetrathiafulvalene (TTF).

powder collected for the subsequent washing treatment to remove the excess dye adsorbed on the matrix outer surfaces: the material prepared was suspended in spectroscopic-grade CH_2Cl_2 (Fluka) and put into an ultrasonic bath for 10 min. After centrifugation (6 min at 5000 rpm), the supernatant solution was removed and the dye content in the solution evaluated by PL spectroscopy. The washing was repeated until the intensity of the collected PL signal becomes negligible.
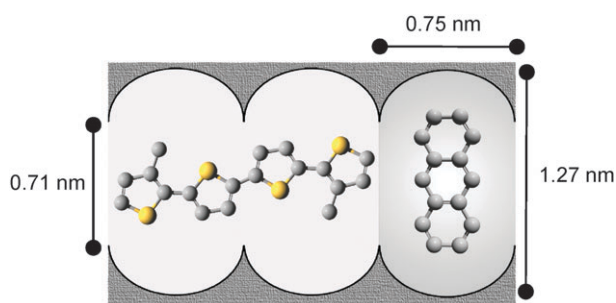
Optical data acquisition

Absorption and PL spectra at room temperature (RT) were collected with a Varian Cary 50 Scan spectrophotometer (bandwidth 1 nm) and a Varian Cary Eclipse spectrofluorometer (bandwidth 1 nm), respectively. Low-temperature (LT) PL and PL excitation (PLE) measurements were performed in a bath cryostat using a monochromated Xe lamp as excitation source (bandwidth 1 nm), and a N_2-cooled CCD camera coupled with a 190 nm polychromator (bandwidth 0.5 nm) for signal detection. For time-resolved PL, the second harmonic of a Ti:sapphire laser (Coherent MIRA 900) was used to provide a pulsed excitation and a Chromex 250is spectrometer coupled to an Hamamatsu streak camera for the detection of the PL time evolution (the overall time resolution was a few picoseconds). Fluorescence quantum yields on dilute solutions were measured by using quinine sulfate as reference. For solid state materials, the measurements were carried out with a home-made integrating sphere. Microscope images of single LTL crystals were collected with an Olympus FluoView 300 confocal microscope. All the optical measurements were corrected for the instrumental spectral responses.

Results and discussion

This section has been divided into three subsections, discussing separately the main aspects of this investigation: PL properties of HGCs, role of the host matrix, and role of the loaded guest. In the first part, the occurrence of peculiar PL emission in DM4T-loaded LTL material is detailed along with additional measurements performed in order to rule out phenomena not involving host–guest interactions that could also explain the observed behavior like solid-state aggregation, self-absorption, interaction with atmosphere (water, oxygen), chemical moisture, migration of the excitation. The second part deals with the surrounding matrix and investigates the impact of the presence or absence of free cations in the host framework. In the third part, the nature of the organic chromophore is under the spotlight and its geometrical (planarity, permanent dipole moment) and chemical features (presence of sulfur atoms) are considered. The last part establishes a simple quantum-chemical scheme to rationalize the experimental observations.

Red-shifted emission in DM4T-loaded LTL

Among zeolites with cavities large enough to accommodate an organic dye, LTL has been chosen because of its versatility in HGC preparation[26] and its peculiar geometrical and chemical features. The one-dimensional channels running through the whole crystal (see Scheme 2) and the charge-compensating counter-ions (due to Al atoms in the framework) make LTL a

Scheme 2 Scheme of LTL channel along with the arrangement of (i) DM4T occupying 2 unit cells (left) and (ii) ANT (right) fitting 1 unit cell.

model material to investigate the interaction between cations and rod-like chromophores.

Successful chromophore loading in LTL has been proven by fluorescence microscopy images. As depicted in Fig. 1(a), emission under UV light is detected at room temperature from the inside of a single cylindrical-shaped crystal of DM4T-LTL. Moreover, the crystal emission is mainly polarized parallel to the main LTL crystal axis, and thus to the channel axis, since the crystal PL is only barely detectable when the perpendicular component of the emission is collected. This finding suggests that the angle between the DM4T transition dipole moment and the channel main axis is close to zero. Since the transition dipole moment of the S_1–S_0 transition in thiophene oligomers is nearly parallel to the long molecular axis,[27] this implies that the DM4T molecules are essentially aligned along the LTL channels, as expected by considering the constraints imposed by the channel geometry that prevent the herringbone-like packing typical of OTs in the solid state.

In Fig. 1(b) the low-temperature PL spectrum of a DM4T dilute solution ($\leq 10^{-5}$ M) in CH_2Cl_2 is compared to those of DM4T-LTL samples with different DM4T loading levels (DM4T-LTL-H and DM4T-LTL-L, with nominal loadings of 100% and 20%, respectively), recorded at 77 K. The PL spectrum of the DM4T dilute solution shows a vibronic progression characterized by an energy separation of about 0.18 eV, in good agreement with the energy of the vibrational modes strongly coupled to the lowest electronic transition in oligothiophenes.[28,29] The origin of the vibronic progression, corresponding to the pure (adiabatic) electronic transition S_1–S_0, is at 2.75 eV and is referred to as the 0–0 transition of the isolated molecule. The HGCs PL spectra also show for both samples a vibronic progression with the typical $\sim$0.18 eV energy separation though the origin of the progressions is at 2.65 eV, regardless the amount of loaded DM4T. The peaks are somewhat broader than those of the dilute (frozen) solution, probably due to the more inhomogeneous chemical environment experienced by the chromophores within the LTL channel.

The spectroscopic data collected for the DM4T dilute solution and DM4T-LTL-H sample, including PL quantum yields (Φ_F) and lifetimes (τ_{tot}) measured at room temperature, are reported in Table 1. The non-radiative rate (k_{nr}), which accounts for all non-radiative decay processes, has been calculated by using the standard relation:[30] $k_{nr} = (1 - \Phi_F)/\tau_{tot}$. The low PL efficiency of
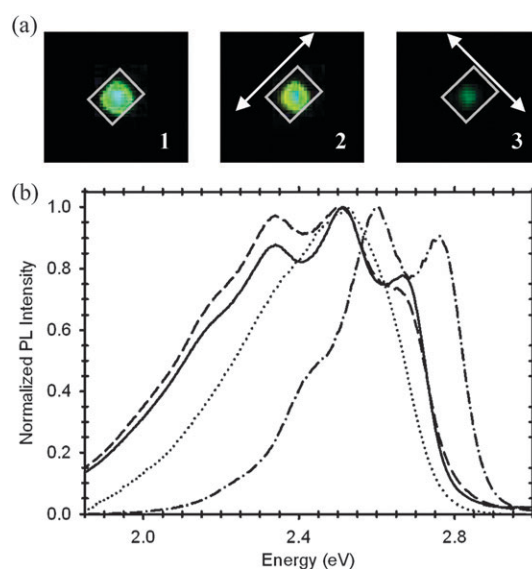

Fig. 1 (a) Room-temperature fluorescence microscopy images of a single zeolite microcrystal of DM4T-LTL-H sample, (1) without polarizer, (2) and (3) with polarizer where the direction of the transmitted polarization is indicated by the arrows (the rectangles show overall shape of the crystal with its main axis co-linear with the arrow in (2). (b) Comparison between PL spectra of DM4T-LTL-H (solid line), DM4T-LTL-L (dashed line), DM4T-LTL-Ox (dotted line) and DM4T dilute solution in CH_2Cl_2 (dash-dotted line) collected at 77 K.

less than 2% could be ascribed to the electric field induced by the cations in the channels,[31] which is known to increase in polymers and molecules the distance between the center of gravity of the positive and negative excitonic charges, therefore enhancing the probability of dissociation of the excitation.[32–34]

To understand the unusually large PL red-shift of 0.1 eV against solution observed in our system regardless of dye concentration (see also the ESI†), we first investigated possible 'trivial' reasons including self-absorption, a change in the refractive index, interactions with atmosphere (O_2 and H_2O vapor), as well as aggregation or polaron formation. Self-absorption can indeed be large in the high-energy part of the PL spectrum, while the impact on the position of the $0 - n$ replica for $n > 0$ becomes increasingly negligible, even for high dye concentrations. In Fig. 2, PL spectrum of DM4T-AlPO-5, with a dye-loading in the same range of DM4T-LTL samples, is perfectly superimposed to that of DM4T dilute solution, demonstrating the trifling effect of self-absorption. This

Table 1 Electronic origin (E_{00}) of PL spectra, luminescence quantum yield (Φ_F), total lifetime (τ_{tot}),* radiative (k_{rad}) and non-radiative (k_{nr}) rates for DM4T dilute solution in CH_2Cl_2 and DM4T-LTL-H sample at room temperature

	DM4T in CH_2Cl_2	DM4T-LTL-H
E_{00}	2.75 eV	2.65 eV
Φ_F	0.19	<2%
τ_{tot} ^{a}	400 ps*	100 ps*
k_{rad} ^{a}	4.8×10^8 s^{-1}	$< 2.0 \times 10^8$ s^{-1}
k_{nr} ^{b}	2.0×10^9 s^{-1}	$\sim$$1.0 \times 10^{10}$ s^{-1}

^{a} Calculated from Φ_F and τ_{tot}. ^{b} Calculated from τ_{tot} and k_{rad}.

This journal is © the Owner Societies 2010

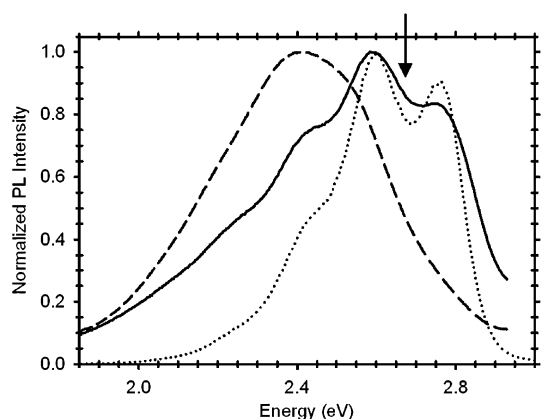*Phys. Chem. Chem. Phys.*, 2010, **12**, 2599–2605 | **2601**

Fig. 2 PL spectra of DM4T-ETS (dashed line) and DM4T-AlPO-5 (solid line) compared with DM4T dilute solution in CH2Cl2 (dotted line) collected at 77 K. Arrow indicates 0–0 transition in DM4T-LTL samples.

situation is very different from the PL of DM4T-LTL-H and -L which show a rigid red-shift of the whole progression compared to DM4T dilute solution PL.

As a further possible reason for the PL red-shift, the refractive index of zeolite (n = 1.5) should be taken into account, affecting the spectral position mainly *via* the oscillator strength. However, the spectral shift against CH_2Cl_2 solution is expected to be rather small ($|\Delta E| \leq 0.02$ eV).[35,36] Indeed, distyrylbenzene (which has an oscillator strength comparable to 4T) adsorbed on silica displayed no visible red-shift compared to dilute solution.[8] Thus, the polarizability of the zeolite is not held responsible for the observed PL shift.

The PL spectra are known to be also affected by adsorbed water molecules as well as photo-degradation due to oxygen contamination, *e.g.* after HGC preparation. In order to verify that the red shift is already present before air exposure, PL measurements have been performed on a sample (DM4T-LTL-Ox) inside the sealed glass ampoule in which the HGC is prepared. The detected emission is reported in Fig. 1(b). The DM4T-LTL-Ox PL spectrum (dotted line) shows a featureless broad band with a maximum at about 2.5 eV: the lack of the vibronic progression can be ascribed to an inhomogeneous broadening due to chromophores adsorbed not only inside the zeolite crystals but also on the zeolite outer surfaces or on the glass ampoule inner walls. The overall shift of the PL spectrum is quite similar to that in DM4T-LTL-H besides a strong reduction of the 0–0 feature, which is most probably due to self-absorption. Thus, the oxygen/water free sample preparation procedure did not prevent the PL red shift.

Aggregation also may red-shift the PL emission spectra of thiophenes. Herringbone aggregate formation, which is observed for unsubstituted or methyl-substituted 4T molecules,[37–39] and which leads to shifts of typically −0.2 eV,[40] is not possible in the constrained framework of LTL. A "tilted-card-pack" arrangement with (partial) overlap of the π-system of two chromophores can, in principle, occur.[41] However, the fact that shifted PL is also observed in samples with very low dye concentration (see ESI†) rules out aggregation as responsible for the shift of the emission spectrum. Moreover, if
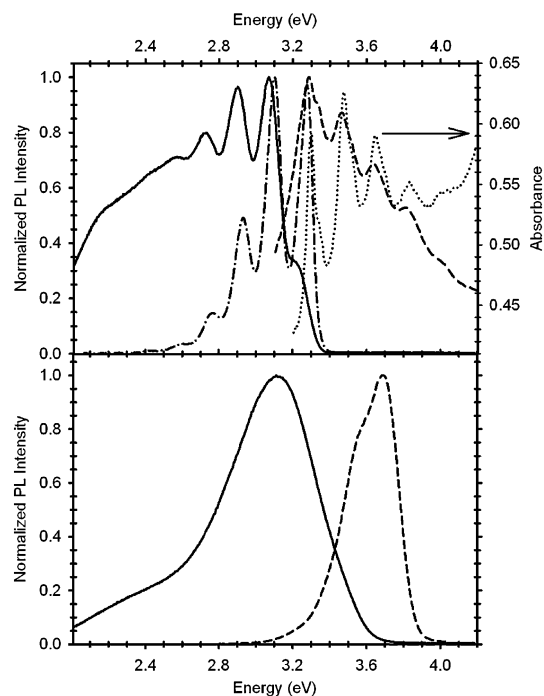

Fig. 3 Top: PL and PLE spectra of ANT-LTL (solid and dashed line, respectively) compared with emission and optical absorption spectra of ANT dilute solution in EtOH (dash-dotted and dotted lines, respectively) collected at room temperature. Bottom: PL spectra of DBT-LTL (solid line) compared with emission spectra of DBT dilute solution in CHCl3 (dashed line) collected at room temperature.

the propensity to form such an aggregate is so strong, this predisposition should emerge in all the hosts, which is indeed not the case as described in the next section.

On the other hand, an excimer-like interaction between neighbouring molecules may account for the broad and unstructured PL tail below 2.4 eV whose intensity increases as the dye concentration does (see ESI†). Although the formation of OTs excimers is rather uncommon (especially for substituted ones), this behavior has been reported in porous hosts for ANT (see Fig. 3),[2,10] and in a spatially constrained OTs scaffold.[42] Finally, we can also exclude the formation of radical cations (polarons) as a possible source of the PL shift, since the polaron features should be found at much smaller energies ($\sim$1.1 eV) than the features observed in the present case.[43] In summary, the data obtained demonstrate that the main emission band in DM4T-LTL samples, shifted with respect to the solution, is due to the monomeric emitting species.

Role of the host framework

After excluding self-absorption, polarizability, atmosphere interactions, as well as aggregation or polaron formation as a possible source for PL red shift, we thus attribute the effect to the specific interaction with the host matrix. As mentioned above, the presence of Al atoms in the LTL crystalline structure is compensated by counter-ions (*i.e.*, K$^+$ ions) within its framework. The peculiar behavior of cation-rich porous oxides has been evaluated by choosing two other hosts,

2602 | *Phys. Chem. Chem. Phys.*, 2010, **12**, 2599–2605

This journal is © the Owner Societies 2010

namely ETS and AlPO-5 (both having geometrical constraints similar to those of LTL), which differ mainly by the presence (Na^+ and K^+ in ETS) or absence (AlPO-5) of charge-compensating cations. In Fig. 2, the PL spectra of DM4T-ETS and DM4T-AlPO-5 measured at 77 K are reported and compared with that of the DM4T dilute solution in CH_2Cl_2 recorded at 77 K. The DM4T-ETS emission is characterized by a broad band centered at about 2.45 eV. The lack of vibronic structures can be ascribed to the polymorphic nature of the titanosilicate host matrix: guest molecules can thus experience a larger number of local environments compared to crystalline zeolite structures, leading to a broadening of the vibronic replica and hence to an unstructured PL. Comparing the center of gravity of the emission spectra, a red shift of about 0.2 eV is observed against the DM4T dilute solution, not so different from the situation in LTL.

On the contrary, as mentioned before, in the case of the cation-free DM4T-AlPO-5 HGC, the PL spectrum shows a vibronic progression (with the typical 0.18 eV energy separation) whose origin (0–0 transition) at 2.76 eV is perfectly superimposed with that of the DM4T dilute solution, so that ALPO-5 can be considered as a rather unspecific host material.

Summing up the results above, the occurrence of a red-shifted emission is detected only in hosts that contain positive counter-ions in their structure, namely LTL (K^+) and ETS (Na^+ and K^+), while in materials with no free cations, such as AlPO-5, the emission is not shifted compared to solution.

Role of the chromophore

As we have seen above, cations do not only deplete the quantum yield of the material but can also tune the position of the emission band. However, this might critically depend on the nature of the inserted molecule. In order to evidence the role of the sulfur atoms (in particular the softness and plasticity of the C–S bonds in OTs due to the highly polarizable lone-pair electrons),[38,39] LTL materials loaded with three different chromophores have been prepared. In Fig. 3 (top), PL and PL excitation (PLE) spectra of ANT-LTL samples are compared with the PL and optical absorption spectra of ANT in dilute solution, showing both well-resolved vibronic progressions. The spectral positions of the absorption bands of ANT in LTL are very similar to those in dilute solution; thus guest–guest and/or guest–host ground-state interactions are negligible.

In emission, the high energy part of the spectrum in LTL is similar to in solution, though showing significant self-absorption. The high energy features assigned to mono-molecular species show a small red shift of the spectrum against solution (as evidenced from the 0–1 position) about 10 times smaller than the corresponding value observed for DM4T-based samples. These findings demonstrate that ANT is almost unaffected by the LTL chemical environment, in quite good agreement with literature studies on ANT dispersed within NaX cavities reporting almost negligible shifts against the solution spectra.[2,10]

The low-energy part of the ANT-LTL emission is significantly affected by the presence of a structure-less broad band centered at about 2.4 eV which contributes to the rise of high-order replicas. As reported in the literature,[10] porous hosts such as LTL (see Scheme 2) do not prevent the formation of ANT excited dimers even at quite low loadings, leading to the unstructured low-energy PL characteristic of excimers. It should be pointed out that excited-dimer formation of ANT is promoted by its planarity, which allows for an effective overlap of molecular orbitals (π-stacking). Such an interaction is so pronounced that ANT is known to show excimer emission in solution and in different environments.[2,10,30] In the present case, LTL geometry does not prevent this tendency.

In order to validate whether the different behavior displayed by DM4T with respect to ANT is really due to the presence of sulfur atoms, or whether molecular planarity and torsional degrees of freedom may play some role, we have prepared LTL materials loaded with a fully-rigid, sulfur-containing chromophore, i.e. DBT. In Fig. 3 (bottom), the PL spectrum of DBT-LTL is reported with the corresponding spectrum of DBT dilute solution in $CHCl_3$. The PL of the dilute solution shows a slightly structured band with the maximum at 3.7 eV. In the LTL sample, a broad unstructured band centered at 3.1 eV is observed, strongly red-shifted against solution. The broad shoulder at around 2.4 eV is is tentatively assigned to excimer formation. It should be stressed that in contrast to DMe4T, DBT is a non-centro-symmetric molecule, thus possessing a permanent electric dipole moment both in the ground and excited states. It is well-known that these dipoles may interact with a polar environment, such as the one experienced within cation-rich host matrices, leading to solvato-chromic effects in the dye PL emission, i.e., an effect which might induce an additional bathochromic shift. However, it is worth stressing that tetrathiafulvalene (TTF), a sulfur-containing centro-symmetric compound, also experiences a red shift upon inclusion in zeolite NaY,[44] whose cavities have pore entrance diameter and chemical environment similar to LTL.

All together, the results demonstrate the key role played by the sulfur atom inducing bathochromic shifts of the PL in the presence of cation-containing host materials, as summarized in Table 2.

The phenomenon observed can be considered as a specific interaction between the chromophore and a nearby cation. As mentioned above, no hints have been found in the literature about the description of cation–π interaction effects on the energy of ground and excited states. From a thermodynamical point of view, the interaction of cations with the benzene ring is stronger than with the thiophene moiety.[1] In contrast, in our case, the impact of cations on ANT PL (Fig. 3 (top)) is negligible when compared to that observed for sulfur-rich chromophores (Fig. 1(b) and 3 (bottom)). It should be stressed that the confined geometry of host channels plays a prominent role, forcing the dye to be in close contact with the metal cation, irrespective of the stability of such a complex. We know, however, that different charge compensating cations such as the bivalent rare earth or trivalent cations, small organic cations, protons, Tl^+ and others can result in very different properties. Here we focus on potassium as the charge compensating cation and we expect that our results and conclusions are also valid for sodium.

This journal is © the Owner Societies 2010

Phys. Chem. Chem. Phys., 2010, **12**, 2599–2605 | 2603

Table 2 Summary of host–guest materials prepared, along with matrix and chromophore properties and emission red shift reported

Sample	Host	Counterions	Guest	Sulfur atoms	Red-shift
DM4T-LTL	LTL	K^+	DM4T	○	○
DM4T-ETS	ETS-10	Na^+, K^+	DM4T	○	○
DM4T-AlPO-5	AlPO-5	—	DM4T	○	—
ANT-LTL	LTL	K^+	ANT	—	—
DBT-LTL	LTL	K^+	DBT	○	○[a]
TTF[b]	NaY	Na^+	TTF	○	○[b]

[a] Permanent dipole moment must be considered. [b] From literature.[44]

Cation–chromophore interactions: a quantum-chemical insight

In order to better analyze how the proximity of a cation could affect the electronic levels of a given chromophore, we have performed quantum-chemical calculations to estimate the HOMO–LUMO gap of two model systems, representative of sulfur-rich molecules (bithiophene, 2T) and homonuclear aromatic dyes (ANT), in interaction with a potassium-like sparkle charge. Calculations were carried out with the ChemOffice 6.0 package of CambridgeSoft, using the semi-empirical Hartree–Fock PM3 method. We have first optimized the chromophore geometry in a planar conformation (the ANT backbone is rigid while OTs get planarized in the excited state);[45] we have then calculated the evolution of the HOMO–LUMO gap when varying the separation of the sparkle charge. Considering that the Stokes shift of substituted OTs is known to be negligible at low temperature, the evaluation of the trend in HOMO–LUMO energy gap is expected to be a reliable modelization to account for the observed PL shift. The obtained results are plotted in Fig. 4. For 2T, we let the cation approach the chromophore both perpendicularly to the molecular plane (z-axis) and along a direction lying in that plane (x direction). In the first case, calculations have been done for 2T in the cis as well as trans conformations. For ANT, the K-like sparkle was moved in a direction both normal to the molecular plane and parallel to the x-axis, pointing either towards the peripheral hydrogens or the inner C atoms. Inspection of Fig. 4 reveals that, below 0.5 nm (no effects are detected before), the calculated shift for 2T is always much larger than for ANT, regardless of the approaching direction. Even though these calculations have been performed in an oversimplified framework, they further demonstrate the prominent role played by sulfur atoms. Moreover, for distances around 0.3 nm, comparable with those between the chromophores and the cations in LTL channels (van der Waals radii of C, S, and K^+ of 0.17, 0.18, and 0.15 nm, respectively), the calculated red shifts for both 2T and ANT are of the same order of magnitude as the experimental values obtained for DM4T-LTL-H and ANT-LTL samples. It should be pointed out that this estimation is of course merely qualitative. In order to have a more precise evaluation, the shielding effect on cations due to the LTL framework should be taken into account, as well as the number of cations actually in proximity to the included dye (DM4T spans two unit cells, see Scheme 2, therefore having access to at least 3 K^+). The theoretical approach thus supports the hypothesis that sulfur atoms are sensitive to the presence of nearby cations; this is probably due to their easily polarizable
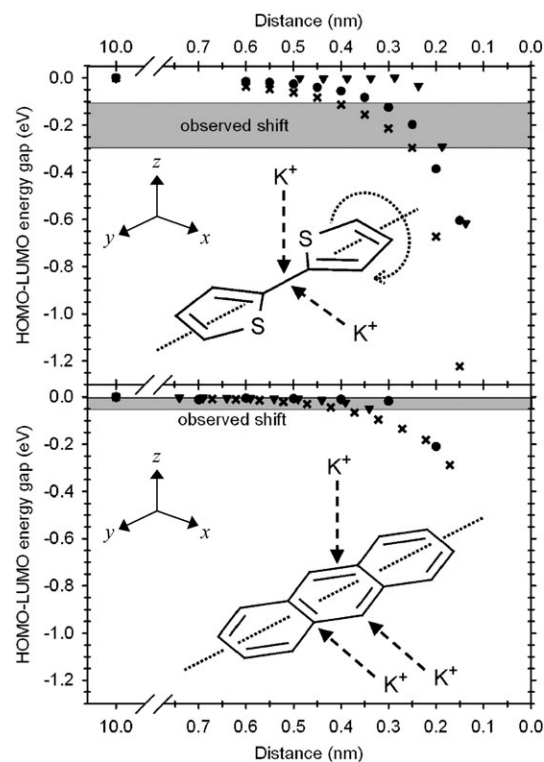

Fig. 4 Calculated energy shift of the HOMO–LUMO gap as a function of the distance between a potassium-like sparkle charge and the chromophore. Top: K+ approaching inter-ring bond of 2T along z-axis (●), along x direction with the dye in cis (▼) and trans (×) conformation. Bottom: K+ approaching long molecular axis of ANT along z-axis (●) and within the molecular plane, pointing towards peripheral H atom (▼) and inner C atom (×). All the distances are considered with respect to the long molecular axis (y-direction). The 0 value in the vertical axis corresponds to the HOMO–LUMO energy gap of the isolated dye molecule (infinite distance).

unpaired electrons and leads to the red-shifted PL observed for sulfur-rich molecules close to cations.

Conclusions

In this work, we employed nanoporous matrices as a tool to force specific dyes to stay in close proximity with cations and to study the interaction between these cations and organic molecules without the necessity to form stable complexes. Besides well-known effects, such as the reduction of the emission efficiency in the presence of large electric fields, we show that the emission energy of sulfur-containing organic

molecules is modulated by the presence of the cations. The observed phenomenon has been carefully verified to be an intrinsic property of the host framework interacting with the guest molecules. The specificity of the presence of both free potassium cations within the matrix and sulfur atoms in the dye backbone has been confirmed by the preparation of various HGCs with different hosts and guests. We found that the shift of the PL emission originates from the easily polarizable lone-pair electrons of the sulfur atoms, as supported by the experimental observations and by quantum-chemical calculations.

Acknowledgements

Notes and references

1 J. C. Ma and A. Dougherty, *Chem. Rev.*, 1997, **97**, 1303.
2 S. Hashimoto, S. Ikuta, T. Asahi and H. Masuhara, *Langmuir*, 1998, **14**, 4284.
3 G. W. Gokel, S. L. De Wall and E. S. Meadows, *Eur. J. Org. Chem.*, 2000, 2967.
4 V. Ramamurthy, J. Shailaja, L. S. Kaanumalle, R. B. Sunoj and J. Chandrasekhar, *Chem. Commun.*, 2003, 1987.
5 A. G. Bezus, A. V. Kiselev and P. Q. Du, *J. Colloid Interface Sci.*, 1972, **40**, 223.
6 D. Oelkrug, S. Uhl, M. Gregor, R. Lege, G. Kelly and F. Wilkinson, *J. Mol. Struct.*, 1990, **218**, 435.
7 H.-J. Egelhaaf, M. Brun, S. Reich and D. Oelkrug, *J. Mol. Struct.*, 1992, **267**, 297.
8 D. Oelkrug, W. Flemming, R. Füllemann, R. Günther, W. Honnen, G. Krabichler, M. Schäfer and S. Uhl, *Pure Appl. Chem.*, 1986, **58**, 1207.
9 A. Devaux, C. Minkowski and G. Calzaferri, *Chem.–Eur. J.*, 2004, **10**, 2391.
10 S. Hashimoto, M. Hagiri, N. Matsubara and S. Tobita, *Phys. Chem. Chem. Phys.*, 2001, **3**, 5043.
11 R. Q. Albuquerque and G. Calzaferri, *Chem.–Eur. J.*, 2007, **13**, 8907.
12 B. Bussemer, I. Dreiling, U.-W. Grummt and G. J. Mohr, *J. Photochem. Photobiol., A*, 2009, **204**, 90.
13 V. Ramamurthy, Photoproceseses of organic molecules included in zeolites, in *Photochemistry in Organized and Constrained Media*, ed. V. Ramamurthy, VCH publishers, New York, 1991, pp. 429–493.
14 J. V. Caspar, V. Ramamurthy and D. R. Corbin, *Coord. Chem. Rev.*, 1990, **97**, 225.
15 G. Calzaferri, S. Huber, H. Maas and C. Minkowski, *Angew. Chem., Int. Ed.*, 2003, **42**, 3732.
16 P. J. Langley and J. Hulliger, *Chem. Soc. Rev.*, 1999, **28**, 279.
17 M. Aloshyna, B. Milián Medina, L. Poulsen, J. Moreau, D. Beljonne, J. Cornil, G. Di Silvestro, M. Cerminara, F. Meinardi, R. Tubino, H. Detert, S. Schrader, H.-J. Egelhaaf, C. Botta and J. Gierschner, *Adv. Funct. Mater.*, 2008, **18**, 915.
18 L. Poulsen, M. Jazdzyk, J.-E. Communal, J. C. Sancho-García, A. Mura, G. Bongiovanni, J. Cornil, M. Hanack, H.-J. Egelhaaf and J. Gierschner, *J. Am. Chem. Soc.*, 2007, **129**, 8585.
19 R. Hoss, O. Konig, V. KramerHoss, U. Berger, P. Rogin and J. Hulliger, *Angew. Chem., Int. Ed. Engl.*, 1996, **35**, 1664.
20 G. Schulz-Ekloff, D. Wöhrle, B. van Duffel and R. A. Schoonheydt, *Microporous Mesoporous Mater.*, 2002, **51**, 91.
21 A. Corma and H. García, *Eur. J. Inorg. Chem.*, 2004, 1143.
22 C. van Pham, A. Burkhardt, R. Shabana, D. D. Cunnigham, H. B. Mark and H. Zimmer, *Phosphorus Sulfur*, 1989, **46**, 153.
23 G. Calzaferri and S. Megelski, *Adv. Funct. Mater.*, 2001, **11**, 277.
24 C. C. Pavel, D. Vuono, L. Catanzaro, P. De Luca, N. Bilba, A. Nastro and J. B. Nagy, *Microporous Mesoporous Mater.*, 2002, **56**, 227.
25 I. Girnus, M. M. Pohl, J. Richtermendau, M. Schneider, M. Noack, D. Venzke and J. Caro, *Adv. Mater.*, 1995, **7**, 711.
26 G. Calzaferri and K. Lutkouskaya, *Photochem. Photobiol. Sci.*, 2008, **7**, 879.
27 F. Meinardi, M. Cerminara, A. Sassella, A. Borghesi, P. Spearman, G. Bongiovanni, A. Mura and R. Tubino, *Phys. Rev. Lett.*, 2002, **89**, 157403.
28 D. Birnbaum, D. Fichou and B. E. Kohler, *J. Chem. Phys.*, 1992, **96**, 165.
29 B. Milián Medina, D. Wasserberg, S. C. J. Meskers, E. Mena-Osteritz, P. Bäuerle and J. Gierschner, *J. Phys. Chem. A*, 2008, **112**, 13282.
30 J. B. Birks, *Photophysics of Aromatic Molecules*, Wiley, 1970.
31 R. Kahn, E. Cohen De Lara and K. D. Möller, *J. Chem. Phys.*, 1985, **83**, 2653.
32 M. C. J. M. Vissenberg and M. J. M. de Jong, *Phys. Status Solidi B*, 1998, **205**, 347.
33 Y. Hou, X. Yang, Y. Li and X. Xu, *Thin Solid Films*, 2000, **363**, 248.
34 M. I. Khan, G. C. Bazan and Z. D. Popovic, *Chem. Phys. Lett.*, 1998, **298**, 309.
35 H.-J. Egelhaaf, J. Gierschner and D. Oelkrug, *Synth. Met.*, 2002, **127**, 221.
36 J. Gierschner, H.-J. Egelhaaf, H.-G. Mack, S. Schweizer, B. Doser and D. Oelkrug, *Synth. Met.*, 2003, **138**, 311.
37 M. Pope and C. E. Swenberg, *Electronic Processes in Organic Crystals and Polymers*, Oxford University Press, 2nd edn, 1999.
38 G. Barbarella, M. Zambianchi, A. Bongini and L. Antolini, *Adv. Mater.*, 1992, **4**, 282.
39 G. Barbarella, M. Zambianchi, A. Bongini and L. Antolini, *Adv. Mater.*, 1993, **5**, 834.
40 J. Gierschner, J. Cornil and H.-J. Egelhaaf, *Adv. Mater.*, 2007, **19**, 173.
41 M. Busby, Ch. Blum, M. Tibben, S. Fibikar, G. Calzaferri, V. Subramaniam and L. De Cola, *J. Am. Chem. Soc.*, 2008, **130**, 10970.
42 M. Wroz, J. B. Bombenger, C. Botta, A. Orbelli Biroli, M. Pizzotti, F. de Angelis, L. Belassi, R. Tubino and F. Meinardi, *Chem.–Eur. J.*, 2009, **15**, 12791.
43 J. M. Maud, *Synth. Met.*, 1999, **101**, 575.
44 C. Baehtz, H. Ehrenberg and H. Fuess, *Phys. Chem. Chem. Phys.*, 2000, **2**, 5764.
45 G. Macchi, B. Milián Medina, M. Zambianchi, R. Tubino, J. Cornil, G. Barbarella, J. Gierschner and F. Meinardi, *Phys. Chem. Chem. Phys.*, 2009, **11**, 984.

This journal is © the Owner Societies 2010

Phys. Chem. Chem. Phys., 2010, **12**, 2599–2605 | 2605